Pis'ma v ZhETF, vol. 100, iss. 12, pp. 865 – 869

IceCube astrophysical neutrinos without a spectral cutoff and $10^{15}-10^{17}$ eV cosmic gamma radiation

O. Kalashev, S. Troitsky[1)]

Institute for Nuclear Research of the RAS, 117312 Moscow, Russia

Submitted 11 October 2014

We present a range of unbroken power-law fits to the astrophysical-neutrino spectrum consistent with the most recent published IceCube data at the 68 % confidence level. Assuming that the neutrinos originate in decays of π-mesons, we estimate accompanying gamma-ray fluxes for various distributions of sources, taking propagation effects into account. We then briefly discuss existing experimental results constraining PeV to EeV diffuse gamma-ray flux and their systematic uncertainties. Several scenarios are marginally consistent both with the KASKADE and CASA-MIA upper limits at 10^{15}–10^{16} eV and with the EAS-MSU tentative detection at $\sim 10^{17}$ eV, given large systematic errors of the measurements. Future searches for the diffuse gamma-ray background at sub-PeV to sub-EeV energies just below present upper limits will give a crucial diagnostic tool for distinguishing between the Galactic and extragalactic models of the origin of the IceCube events.

DOI: 10.7868/S0370274X14240011

The observation of an excess of high-energy neutrinos above the atmospheric background by the IceCube observatory [1–3] gave a strong boost to astroparticle physics (see, e.g., Ref. [4] for a review and references). While a firm conclusion about the astrophysical origin of these events would require future studies and a confirmation by an independent experiment, numerous scenarios have been put forward to explain the observation. Not surprisingly, present low statistics does not allow to single out a unique explanation of the origin of these events.

Absence of observed events with energies $E \gtrsim 3\,\mathrm{PeV}$ is often considered as an argument for the presence of a spectral cutoff at these energies. Indeed, the experimental exposure for electron antineutrinos peaks around $\sim 6.3\,\mathrm{PeV}$ because of the Glashow resonance, and one would expect additional events while none is detected (see, e.g., Ref. [5] for a detailed discussion). This cutoff would add further uncertainty to astrophysical explanations because the maximal energy of 3 PeV is not singled out by any general argument. In this note, we assume that the neutrino spectrum continues beyond the highest observed energies and the absence of events at the Glashow resonance is a statistical fluctuation, not an indication of a cutoff. We will see that this assumption agrees with the data perfectly.

The general conventional model for production of energetic astrophysical neutrinos implies their creation in decays of charged π-mesons, $\pi^{\pm}$, produced in turn in high-energy hadronic or photohadronic interactions. These $\pi^{\pm}$'s are necessary accompanied by neutral π^0's which decay to photons. The energetic photons, therefore, have to accompany energetic neutrinos, see e.g. Refs. [6, 7] for discussions and estimates and Refs. [8–10] for more detailed model analyses in the context of the IceCube result. Since the neutrinos propagate freely through the Universe while the photons may be absorbed, a comparison of the two fluxes may give important information about the distribution of sources. In what follows, we will estimate the gamma-ray flux expected in various scenarios, starting from the IceCube data. Throughout the paper, we will assume that:

- the neutrino spectrum follows an unbroken power law,
$$\frac{dF}{dE} = N \left(\frac{E}{\mathrm{TeV}}\right)^{-\alpha}, \qquad (1)$$
where the diffuse flux F is measured in $\mathrm{cm}^{-2} \times \mathrm{s}^{-1} \times \mathrm{sr}^{-1}$;
- all neutrinos originate from $\pi^{\pm}$ decays, and the mechanism producing these $\pi^{\pm}$'s provides for equal amounts of π^+, π^-, and π^0;
- the neutrino mixing is maximal, so, given previous assumptions, the neutrinos arrive to the observer with $1:1:1$ flavor ratio.

Deviations from these assumptions are certainly present but their account is beyond the precision of the present data.

[1)]e-mail: st@ms2.inr.ac.ru

To proceed, we first need to quantify the astrophysical neutrino flux consistent with observations. This part of the study may be useful for other phenomenological considerations, so we discuss it in some detail.

IceCube reported 37 high-energy astrophysical neutrino candidate events at the background expectation of ~ 15. This small statistics is expected to agree with various descriptions of the spectrum. The original IceCube paper [3] does not present a range of allowed spectral fits and quotes only two benchmark fits, one with fixed $\alpha = 2.0$ and the best fit with $\alpha = 2.3$. However, all necessary information to obtain the allowed region of parameters (N, α) at a given confidence level is published, and we will use it in this study. Namely, the energies of 36 of the observed events and the energy-dependent number of background events are given in Ref. [3] while the energy dependence of the exposure is presented in Ref. [7]. There are however two subtle points in the fitting procedure.

Firstly, the number of events in the sample, and especially in high-energy bins, is so small that the standard chi-square method would give a biased result, and the binned Poisson likelyhood does not follow the chi-square distribution. This is easy to cure, however, with the Monte-Carlo procedure described e.g. in Ref. [11], which is used here.

Secondly, individual neutrino energies cannot be measured and it is only the deposited energy in the ice which is reported. For cascade events (to which three highest-energy ones belong), the difference between the two energies may be neglected, while for track events the deposited energy gives only a lower limit on the true neutrino energy, which may be several times higher [12]. However, the present IceCube data allow for a nice trick to overcome this problem, suggested in Ref. [7]. It exploits the fact that, occasionally or not, there are no observed events with $400\,\text{TeV} \lesssim E \lesssim 1\,\text{PeV}$, while all three events above 1 PeV are showers. This means that, no matter shower or track, the energies of all neutrinos except these three do not exceed 1 PeV. We therefore adopt the approach of Ref. [7] and use only three bins in the analysis: $E < 1\,\text{PeV}$, $1\,\text{PeV} < E < 2\,\text{PeV}$, and $E > 2\,\text{PeV}$. We use events with $E > 40$ TeV in the fits.

The allowed ranges of the spectral fits are presented in Figs. 1 and 2. The best-fit values are:

$$\alpha = 2.4, \quad N = 8.7 \cdot 10^{-8}\ \text{TeV}^{-1} \cdot \text{cm}^{-2} \cdot \text{s}^{-1} \cdot \text{sr}^{-1}, \quad (2)$$

only slightly different from the best fit of Ref. [3] (the difference may originate in the data included in the fit, $E > 40\,\text{TeV}$ vs. $E > 60\,\text{TeV}$, and in some details of the fitting procedure which is not described in Ref. [3]).

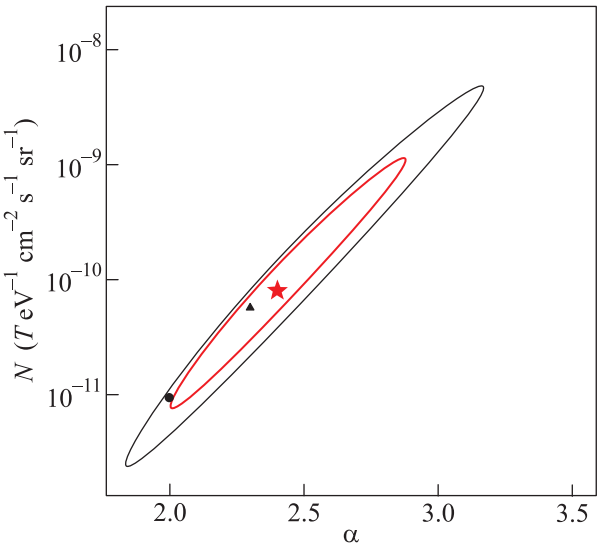

Fig. 1. (Color online) The parameter space (normalization N versus spectral index α) for unbroken power-law fits, Eq. (1), of the astrophysical neutrino spectrum. The thick and thin contours bound the regions of parameters consistent with the IceCube data [3] at the 68 and 95 % C.L., respectively. The star denotes our best-fit value, Eq. (2). The triangle and the circle denote benchmark fits of Ref. [3] with $\alpha = 2.3$ and 2.0, respectively

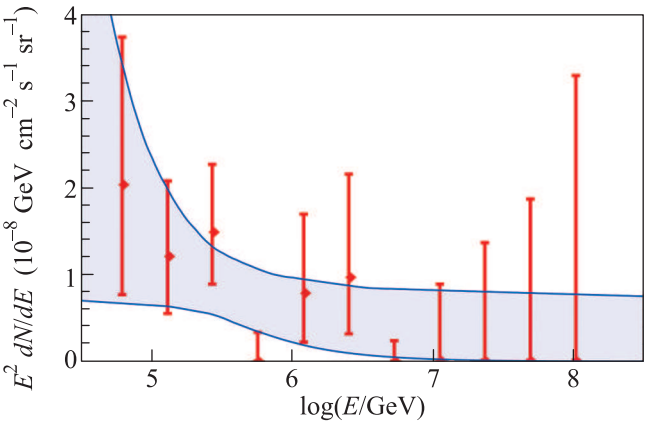

Fig. 2. (Color online) The IceCube astrophysical neutrino spectrum [3] (data points) together with the range of 68 % C.L. allowed power-law fluxes determined in Fig. 1 (shadow)

The data are well described by a power law without any cutoff for a wide range of spectral indices.

Within our assumptions, it is easy to estimate the accompanying flux of photons from π^0 decays. A simple estimate of the gamma-ray flux injected by an optically thin source is given by [4, 13]

$$\left.\frac{dF_\nu^{(i)}}{dE_\nu}\right|_{E_\nu = E_\gamma/2} = 2\left.\frac{dF_\gamma}{dE_\gamma}\right|_{E_\gamma},$$

where $F_\nu^{(i)}$ and F_γ are the fluxes of neutrino (per flavor, that is 1/3 of the total neutrino flux within our assumptions) and photons at energies E_ν and E_γ, respectively.

On their way from the source to the observer, energetic gamma rays participate in electromagnetic cascades, driven by the electron-positron pair production on cosmic background radiations (the relevant contributions here come from the cosmic microwave, infrared and ultraviolet backgrounds, depending on the gamma-ray energies) and by the inverse Compton scattering of electrons and positrons, which produces secondary energetic photons. Therefore, besides gamma rays from π^0 decays, also electrons and positrons from $\pi^\pm$ decays contribute to the cascade and should be taken into account (their contribution is more important for lower-energy, <PeV, part of the observed spectrum and for hard spectral indices). The injected flux F_e of electrons and positrons at the energy E_e is equal to neutrino (per flavour) flux, in the same approximation:

$$\left.\frac{dF_e}{dE_e}\right|_{E_e=E_\nu} = \left.\frac{dF_\nu}{dE_\nu}\right|_{E_\nu}.$$

The photon attenuation length [14] is as short as $\sim 10\,\mathrm{kpc}$ for PeV photons, increasing rapidly at both lower and higher energies. Therefore, mostly Galactic sources may contribute to the gamma-ray flux at PeV–EeV energies, and the observed spectrum of these gamma rays is very sensitive to the distribution of sources in the Galaxy and in its immediate neighbourhood. In what follows, we use publicly available transport equation based code written by one of us [15, 16] to simulate electron-photon cascade propagation. In the case of Galactic source distribution for simplicity we neglect interactions of photons with Galactic infrared and optical backgrounds. This may lead to at most 5 % error in the γ-ray flux predictions in the energy range $30\,\mathrm{TeV} < E_\gamma < 300\,\mathrm{TeV}$ only. We also take into account synchrotron losses of electrons in the $\sim 10^{-6}\,\mathrm{G}$ galactic magnetic field. For the extragalactic infrared and optical background we use the estimate of Ref. [17].

We use several benchmark source distributions $n(\mathbf{r})$ in the Universe. We measure $\mathbf{r} = (x, y, z)$ from the Galactic Center and account for a non-central position of the Sun in the Galaxy (assuming that the Sun is 8.5 kpc from the center).

1. Stellar distribution: assume that $n(\mathbf{r})$ follows the distribution of stars in the Galaxy [18]:

$$n(\rho, z) = \mathrm{const}\left[n_d(\rho, z) + n_h(\rho, z)\right],$$

$$n_h(\rho, z) = f_h \left[\frac{R_{\mathrm{Sun}}}{\sqrt{\rho^2 + (z/q_h)^2}}\right]^{N_h},$$

$$n_d(\rho, z) = n_1(\rho, z, L_1, H_1) + f_f n_1(\rho, z, L_2, H_2),$$

$$n_1(\rho, z, L, H) = \exp\left(\frac{R_{\mathrm{Sun}} - \rho}{L} - \frac{|z| + Z_{\mathrm{Sun}}}{H}\right),$$

where the parameter values are $\rho = \sqrt{x^2 + y^2}$, $R_{\mathrm{Sun}} = 8.5\,\mathrm{kpc}$, $Z_{\mathrm{Sun}} = 2.5\,\mathrm{pc}$, $f_f = 0.12$, $f_h = 0.0051$, $q_h = 0.64$, $N_h = 2.77$, $L_1 = 2.6\,\mathrm{kpc}$, $L_2 = 3.6\,\mathrm{kpc}$, $H_1 = 0.3\,\mathrm{kpc}$, $H_2 = 0.9\,\mathrm{kpc}$, and we assume that the distribution extends up to $r_{\max} = 15\,\mathrm{kpc}$.

2. Dark-matter distribution: use the Navarro–Frenck–White (NFW, Ref. [19]) distribution for $n(\mathbf{r})$, with parameters favoured by Ref. [20] for the Milky Way:

$$n(r) = \frac{\mathrm{const}}{x\,(1+x)^2},$$

where $x = r/R_s$, $R_s = R_v/C_v$, the parameter values are $C_v = 12$ and $R_v = 260$ kpc; the integration is extended up to $r_{\max} = R_v$.

3. Halo hot-gas distribution: the observed neutrinos may originate [8, 21] in interactions of cosmic rays with the hot gas which probably fills the outer (up to hundreds of kiloparsecs!) halo of the Galaxy [22]. For the gas density, we use the Maller–Bullock [23] distribution,

$$n_{\mathrm{gas}} = \mathrm{const}\left[1 + \frac{3.7}{x}\log(1+x) - \frac{3.7}{C_c}\log(1+C_c)\right]^{3/2},$$

$$r < R_c,$$

$$n_{\mathrm{gas}} = \mathrm{const}/r^2, \quad R_c < r < R_v,$$

where $C_c = R_c/R_s$ is the parameter of the gas concentration while other notations are determined for the NFW distribution. We have to convolve this distribution with the assumed cosmic-ray density $n_{\mathrm{CR}}(\mathbf{r})$ to obtain the source distribution,

$$n(\mathbf{r}) = n_{\mathrm{gas}}(\mathbf{r}) n_{\mathrm{CR}}(\mathbf{r}).$$

In our numerical example, we assume, following Ref. [21], $n_{\mathrm{CR}} \propto 1/r$, and $C_c = 1$. Clearly, the both choices are oversimplified; the real distributions of both the hot gas and cosmic rays are much more complicated but unfortunately not firmly known. In particular, both are not expected to be spherically symmetric, and the photon and neutrino fluxes are expected to be anisotropic in a realistic case. Deviations from isotropy, which are present also in other scenarios due to a non-central position of the Sun in the Galaxy, are not discussed here.

4. Extragalactic distribution: this is used for illustrative purposes only and assumes $n = \mathrm{const}$ up to the event horizon. Realistic source distributions are not

continuous and would include the distance to the nearest source as a parameter, thus reducing the expected gamma-ray flux even further.

The results of the calculations are presented in Fig. 3.

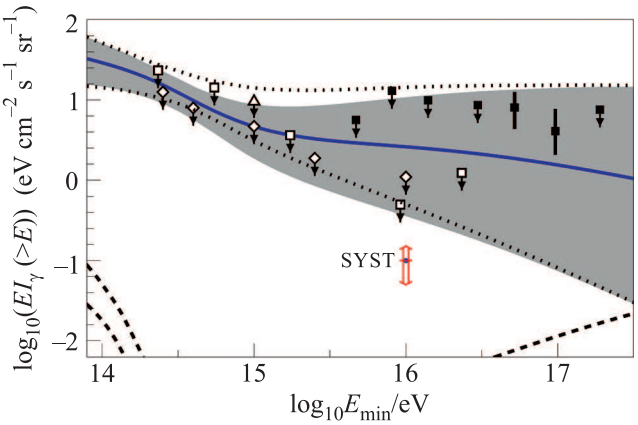

Fig. 3. (Color online) The diffuse cosmic photon integral flux versus the photon minimal energy. The dark shadowed region gives the prediction for the source distribution similar to the hot-gas distribution in the outer halo of the Galaxy and for the 68 % C.L. range of neutrino spectra. The full line (blue online) corresponds to the best-fit neutrino spectrum, Eq. (2), and the same source model. Predictions for the NFW model are similar to the hot-gas model, within the plot precision. Dotted lines bound the range of predictions for the stellar distribution. The light shadowed regions in the lower part (bound by dashed lines) correspond to a uniform extragalactic distribution. Experimental constraints are indicated by symbols: an open triangle (EAS-TOP [24]), open squares (CASA-MIA [25]), open diamonds (KASCADE [26, 27]), and full boxes (EAS-MSU [28, 29]). A range of estimated systematic errors of the upper limits and measurements is indicated by a double arrow (red online)

Several experimental constraints on the gamma-ray flux in the sub-PeV to sub-EeV energy range are available. They are also presented in Fig. 3 and include upper limits from the EAS-TOP [24], KASCADE [26, 27], and CASA-MIA [25] experiments at energies $\sim 0.1-30$ PeV as well as recently published detection claims and upper limits from the EAS-MSU [28, 29] experiment at $\sim 50-500$ PeV. The main source of systematic errors for all these results is related to simulations of the background of photon-like hadronic events, subject to uncertainties of the hadronic interaction models used. It has been estimated in Ref. [28], by comparison of simulations within various models, as ± 50 %. Though this kind of an estimate was not presented in earlier studies (in particular, for the most stringent CASA-MIA limits the publication [25] even does not mention which hadronic model was used for the background estimates), one should expect a similar value of uncertainty for all experimental results presented in Fig. 3[2)]. These large systematic uncertainties may be responsible for the apparent tension between CASA-MIA limits at ~ 10 PeV and EAS-MSU detection claims at > 50 PeV in the context of the scenarios discussed here, so that a certain hard-spectrum model (the hard spectrum is favored also by Refs. [9, 30]) may be consistent with all gamma-ray constraints. Alternatively, a mixture of Galactic and extragalactic contributions may result in a better agreement with data.

In any case, our results suggest that PeV to EeV photons represent a powerful tool to distinguish between models of the origin of IceCube astrophysical neutrinos and to trace the distribution of their sources. Galactic models predict gamma-ray fluxes just below, or at the level of, current observational limits, so searches for primary photons at these energies are more than motivated. In particular, low-energy extensions of large cosmic-ray observatories [31, 32] or dedicated experiments [33] may explore the higher-energy part of the range very soon.

We are indebted to Grigory Rubtsov for interesting and useful discussions and to the EAS-MSU group for sharing the results of Ref. [29] prior to publication. This work was supported by the Russian Science Foundation (grant # 14-12-01340). Numerical calculations have been performed at the computer cluster of the Theoretical Physics Division of the Institute for Nuclear Research of the Russian Academy of Sciences.

1. M. G. Aartsen et al. (IceCube Collaboration), Phys. Rev. Lett. **111**, 021103 (2013); arXiv:1304.5356 [astro-ph.HE].
2. M. G. Aartsen et al. (IceCube Collaboration), Science **342**(6161), 1242856 (2013); arXiv:1311.5238 [astro-ph.HE].
3. M. G. Aartsen et al. (IceCube Collaboration), Phys. Rev. Lett. **113**, 101101 (2014); arXiv:1405.5303 [astro-ph.HE].
4. L. A. Anchordoqui, V. Barger, I. Cholis, H. Goldberg, D. Hooper, A. Kusenko, J. G. Learned, and D. Marfatia, J. High Energy Astrophys. **1–2**, 1 (2014); arXiv:1312.6587 [astro-ph.HE].
5. V. Barger, L. Fu, J. G. Learned, D. Marfatia, S. Pakvasa and T. J. Weiler, arXiv:1407.3255 [astro-ph.HE].

[2)] Note that the uncertainty in the energy estimation, crucial for cosmic-ray studies, is irrelevant here because the energy of a primary gamma ray is determined in a more or less model-independent way.

6. N. Gupta, Astropart. Phys. **48**, 75 (2013); arXiv:1305.4123 [astro-ph.HE].
7. L. A. Anchordoqui, H. Goldberg, M. H. Lynch, A. V. Olinto, T. C. Paul, and T. J. Weiler, Phys. Rev. D **89**, 083003 (2014); arXiv:1306.5021 [astro-ph.HE].
8. M. Ahlers and K. Murase, Phys. Rev. D **90**, 023010 (2014); arXiv:1309.4077 [astro-ph.HE].
9. K. Murase, M. Ahlers, and B. C. Lacki, Phys. Rev. D **88**, 121301 (2013); arXiv:1306.3417 [astro-ph.HE].
10. J. C. Joshi, W. Winter, and N. Gupta, arXiv:1310.5123 [astro-ph.HE].
11. W. H. Press, S. A. Teukolsky, W. T. Vetterling, and B. P. Flannery, *Numerical Recipes: The Art of Scientific Computing*, Cambridge University Press (2007).
12. M. G. Aartsen et al. (IceCube Collaboration), JINST **9**, P03009 (2014); arXiv:1311.4767 [physics.ins-det].
13. L. A. Anchordoqui, H. Goldberg, F. Halzen, and T. J. Weiler, Phys. Lett. B **600**, 202 (2004); astro-ph/0404387.
14. S. Lee, Phys. Rev. D **58**, 043004 (1998); astro-ph/9604098.
15. O. E. Kalashev, V. A. Kuzmin, and D. V. Semikoz, astro-ph/9911035.
16. O. E. Kalashev and E. Kido, arXiv:1406.0735 [astro-ph.HE].
17. T. M. Kneiske, K. Mannheim, and D. H. Hartman, Astron. Astrophys. **386**, 1 (2002); T. M. Kneiske, T. Bretz, K. Mannheim, and D. H. Hartman, Astron. Astrophys. **413**, 807 (2004).
18. M. Juric et al. (SDSS Collaboration), Astrophys. J. **673**, 864 (2008); astro-ph/0510520.
19. J. F. Navarro, C. S. Frenk, and S. D. M. White, Astrophys. J. **462**, 563 (1996); astro-ph/9508025.
20. A. Klypin, H. Zhao, and R. S. Somerville, Astrophys. J. **573**, 597 (2002); astro-ph/0110390.
21. A. M. Taylor, S. Gabici and F. Aharonian, Phys. Rev. D **89** (2014) 103003 [arXiv:1403.3206 [astro-ph.HE]].
22. A. Gupta, S. Mathur, Y. Krongold, F. Nicastro, and M. Galeazzi, Astrophys. J. **756**, L8 (2012); arXiv:1205.5037 [astro-ph.HE].
23. A. H. Maller and J. S. Bullock, Mon. Not. Roy. Astron. Soc. **355**, 694 (2004); astro-ph/0406632.
24. M. Aglietta et al. (EAS-TOP Collaboration), Astropart. Phys. **6**, 71 (1996).
25. M. C. Chantell et al. (CASA-MIA Collaboration), Phys. Rev. Lett. **79**, 1805 (1997); astro-ph/9705246.
26. G. Schatz et al. (KASCADE collaboration), Proc. 28th ICRC, Tsukuba (2003), v. 4, p. 2293.
27. J. Alvarez-Muniz, M. Risse, G. I.Rubtsov, B. T. Stokes for the Pierre Auger, Telescope Array, Yakutsk Collaborations, EPJ Web Conf. **53**, 01009 (2013); arXiv:1306.4199 [astro-ph.HE].
28. Yu. A. Fomin, N. N. Kalmykov, G. V. Kulikov, V. P. Sulakov, and S. V. Troitsky, J. Exp. Theor. Phys. **117**, 1011 (2013); arXiv:1307.4988 [astro-ph.HE].
29. Yu. A. Fomin, N. N. Kalmykov, G. V. Kulikov, V. P. Sulakov, and S. V. Troitsky, Pis'ma v ZhETF **100**, 797 (2014).
30. W. Winter, arXiv:1407.7536 [astro-ph.HE].
31. S. Ogio et al. (Telescope Array Collaboration), *Talk at the International Symposium on Future Directions in UHECR Physics*, CERN, 13–16 February 2012.
32. A. Etchegoyen (Pierre Auger Collaboration), arXiv:0710.1646 [astro-ph].
33. M. Tluczykont, D. Hampf, U. Einhaus, D. Horns, M. Bruckner, N. Budnev, M. Buker, and O. Chvalaev, AIP Conf. Proc. **1505**, 821 (2012).